35th AIAA Plasmadynamics and Lasers Conference
28 June -1 July 2004, Portland, Oregon

AIAA 2004-2565

# Electron Density Measurement of Laser Supported Detonation Waves

*Akio FUKUDA,[1] Yasuro HIROOKA,[2] Koichi MORI,[1] Kimiya KOMURASAKI,[3] and Yoshihiro ARAKAWA[4]*
*The University of Tokyo*
*7-3-1 Hongo, Bunkyo-ku, Tokyo 113-8656, JAPAN*

*Keywords: Laser Propulsion, Laser Supported Detonation, Mach-Zehnder interferometry*

**Abstract**

In Repetitive Pulse laser propulsion, a laser supported detonation (LSD) regime is very important for efficient energy conversion in a vehicle. Then its dependency on operational parameters should be predicted for the vehicle design and its feasibility studies. Electron density distribution behind a shock wave has been measured by means of Mach-Zehnder interferometry. As a result, timing of LSD termination was determined from the history of plasma density discontinuity and the LSD threshold was re-evaluated.

## INTRODUCTION

Recently, air-breathing Repetitively Pulsed (RP) laser propulsion is attracting attentions because it is expected to reduce the launch cost drastically in comparison with existing chemical propulsion systems.

When a high power laser beam is focused in an air, breakdown occurs in the vicinity of the focus. Then, plasma absorbs rest of laser energy and begins to expand while generating a spherical blast wave. The blast wave reflects on the nozzle wall and produces thrust.

Laser Supported Detonation (LSD) wave is known as one of the laser absorption waves. It is accompanied by a shock wave, absorbing laser energy efficiently. The fraction of laser energy that is absorbed by the LSD wave contributes to the thrust, and the rest becomes a frozen flow loss. Therefore, the fractional absorption during the LSD regime is very important for the thrust performance.

The LSD regime will terminate even during laser irradiation because of the decrease in laser intensity on the wave front in a focusing optics. The threshold intensity would be a function of laser energy, pulse duration, ambient pressure, focusing *f*-number, etc.

In this study, the electron density behind the laser-induced blast wave is measured using the Mach Zehnder interferometry. In addition, the fractional laser absorption and LSD threshold are discussed.

## LASER SUPPORTED DETONATION REGIME

Figure 1 shows the shadowgraphs of an exploding blast wave induced by a 10J-$CO_2$-laser.[1] The edge of plasma was recognized identical to the edge of luminous region in each picture, where line and band spectra from the high-temperature air molecules were excluded with the use of band-pass filters. However, the relationship between the luminosity and electron density must be checked.

[1] Graduate Student, Department of Advanced Energy, (e-mail: akio@al.t.u-tokyo.ac.jp)
[2] Graduate Student, Department of Aeronautics and Astronautics,
[3] Associate Professor, Department of Advanced Energy, member AIAA
[4] Professor, Department of Aeronautics and Astronautics, member AIAA

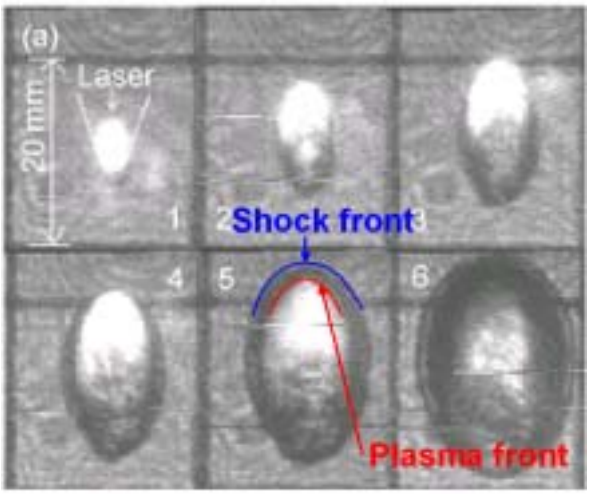


**Fig.1 Shadowgraphs of laser-induced plasma expansion in the atmospheric air, *t*= (1) 0.25μs, (2) 1.0μs, (3) 2.0μs, (4) 3.0μs, (5) 4.0μs, (6) 5.0μs. [1]**

Figure 2 shows the displacements of the shock and plasma fronts from the focus. The coincidence of both fronts occurs during the LSD regime. After $t$≈2.4μs, the shock front propagates further while the plasma front stays behind.

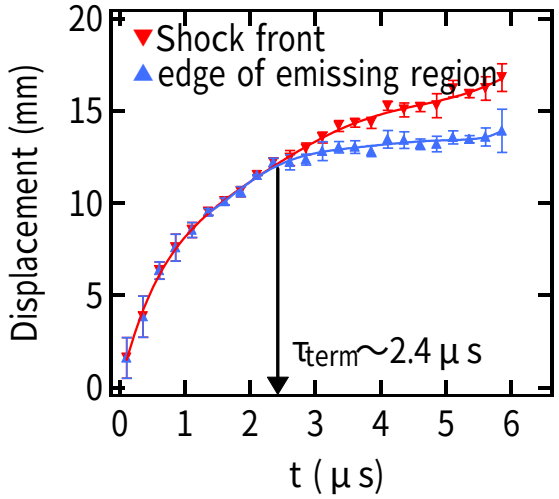


**Fig.2 Displacements of the shock front and plasma front along the laser axis.**

The intersection point of the two curves is considered to be the regime termination timing.

Assuming the quasi-one-dimensional LSD wave propagation as shown in Fig.3, laser intensity $S$ on the LSD wave-surface can be expressed as

$$S = \frac{W}{\pi r_{\mathrm{LSD}}^2} \quad , \qquad (1)$$

where $W$ is the laser power and $r_{\mathrm{LSD}}$ is the radius of the LSD wave-surface front. When the focusing $f$-number of optics is $f$, the relationship between the displacement of the LSD wave $z_{\mathrm{LSD}}$ and $r_{\mathrm{LSD}}$ is expressed as

$$r_{\mathrm{LSD}} = \frac{z_{\mathrm{LSD}}}{2f} \quad . \qquad (2)$$

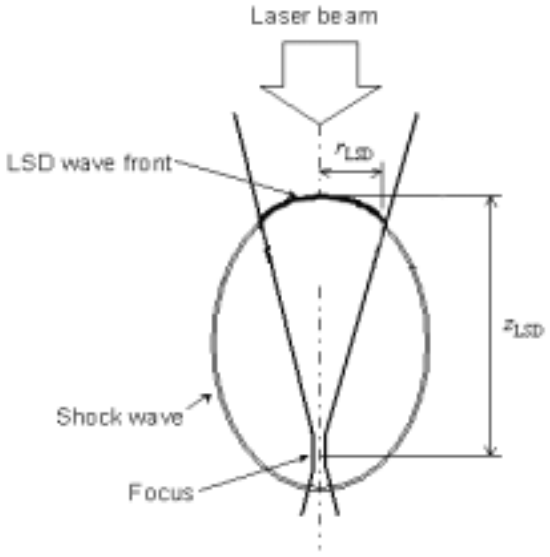


**Fig 3. Schematic of a LSD wave**

Figure 4 shows the measured pulse shape of our 10J TEA $CO_2$ laser using a photon-drag $CO_2$ laser detector (Hamamatsu photonics-B749.) This laser is used in this study and in our previous experiments along with the calculated cumulative energy fraction. $E_i$ is the pulse laser energy. If the LSD regime is terminated at $t$=2.4μs, 90% of $E_i$ has been absorbed in the LSD wave.

The laser intensity threshold on the wave front for the LSD regime has been obtained experimentally as summarized in Table 1. The threshold is increased with $f$ and decreased with $E_i$.

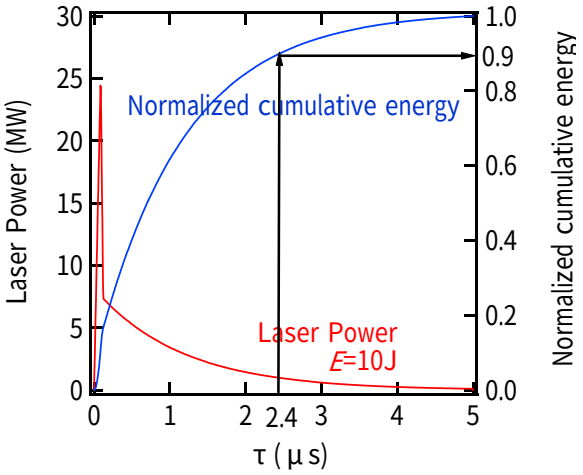


**Fig. 4 Laser pulse shape and cumulative energy.**

**Table 1 LSD threshold for various $E_i$ and focusing *f*-number.[1]**

| $E_i$ (J) | *f* | Threshold (MW/cm$^2$) |
|---|---|---|
| 4 | 1.1 | 6.5 ±0.1 |
| | 2.2 | 7.4 ±0.1 |
| 10 | 1.1 | 2.6 ±0.4 |
| | 2.2 | 3.7 ±0.4 |
| | ∞ | 1 – 10 |

Figure 5 shows the measured blast wave energy; the stagnation enthalpy of the blast wave excluding the chemical potential. It was estimated from the propagation speed of a blast wave during the adiabatic expansion.[2] The blast wave efficiency $\eta_{bw}$ is the ratio of the blast wave energy to $E_i$.

From these measurements, it was concluded that 1) 90% of $E_i$ is absorbed in a LSD wave, and 2) 45% of $E_i$ is used for the blast wave expansion and 45% would be lost as a frozen flow loss.

In order to know the LSD threshold for various operating conditions and to predict the thrust performance of the laser vehicle during the air-breathing flight mode, physics about the LSD wave propagation and termination have to be modeled. For these objectives, electron density measurement is indispensable.

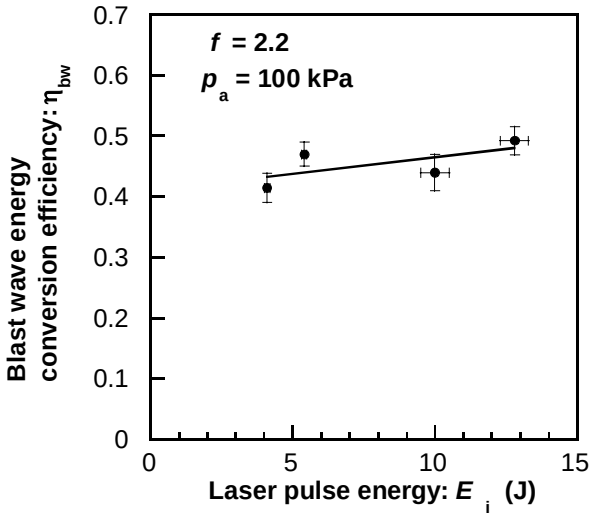


**Fig. 5 Blast wave energy efficiency estimated from the blast wave expansion speed during adiabatic expansion [2]**

## EXPERIMENTAL SETUP

The cross section of the laser beam of our 10-J TEA $CO_2$ laser is a square of 30 × 30mm. The equivalent beam diameter is 34mm, which is the diameter of the circular beam having the same cross-section as the square beam. The laser beam is focused in the air atmosphere using an off-axial parabola mirror. The focal length is 76.2mm and the corresponding focusing *f*-number was 2.2.

Experimental set-up is illustrated in Fig. 6. Pictures of fringe patterns are taken using Image-intensified Change Coupled Device (ICCD) camera (Oriental Instruments InstaSpec™ V ICCD detector, model 77193-5).

An optical emission from a gap switch of a laser discharge tube is utilized to trigger the gate of the camera. A delay-circuit (Stanford Research Systems, Inc. Digital Delay/Pulse Generator Model DG535) transmits a trigger signal to the ICCD camera at an arbitrary timing. He-Ne laser of λ=633nm 12mW CW is used as the light sources. Emission from the plasma is decreased using band-pass filters transmitting wavelength of 633±1nm.

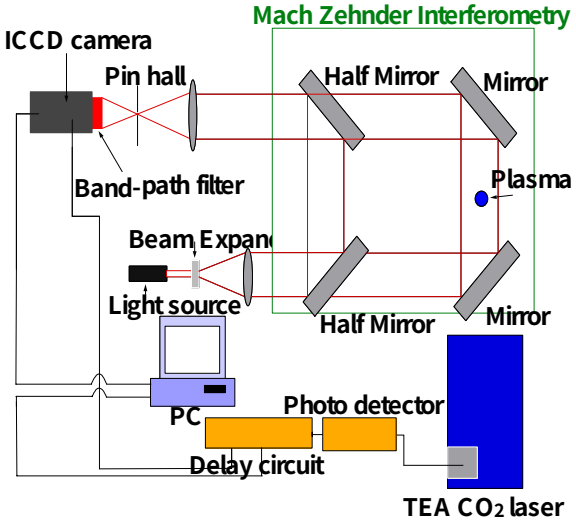


**Fig. 6 Schematic of Mach Zehnder Interferometry system**

## DATA PROCESSING

Fringes aligned in parallel were generated as illustrated in Fig. 7. In the figure, $x$ and $y$ axes indicate the directions parallel and perpendicular to a fringe, respectively. A fringe shift $g(x)$ is defined as a displacement in the $y$-direction from the original fringe line.

When plasma is generated on one path, the fringe pattern varies depending on the change in optical path length. The method of data processing is as follows: The number of the moved fringe line is defined as $g(x)/d$; $d$ is the original interval between the fringes.

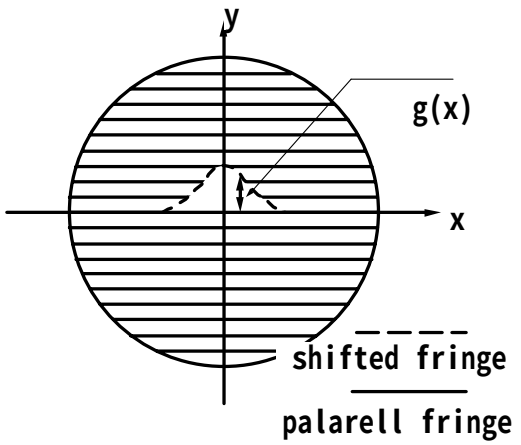


**Fig. 7 Schematic of the parallel and shifted fringe**

The change in the optical path length $\Delta l(x)$ is equal to $\lambda g(x)/d$. $\Delta l(x)$ is also related to the change in the refractive index as the following equation

$$\Delta l(x) = \int_{-z_0}^{z_0} \Delta n(x,z)\mathrm{d}z \qquad (3)$$

where d$z$ is the differential path length.

For axisymmetric plasma, Eq. (3) becomes

$$\Delta l(x) = 2\int_{x}^{R} \frac{r\Delta n(r)}{\left(r^2 - x^2\right)^{1/2}}\mathrm{d}r \qquad (4)$$

Using the Abel inversion, Eq. (4) is transformed to

$$\Delta n(r) = -\frac{\lambda}{\pi}\int_{r}^{R} \frac{\mathrm{d}(g(x)/d)}{\mathrm{d}x}\frac{1}{\sqrt{x^2 - r^2}}\mathrm{d}x \,. \qquad (5)$$

Here, $\Delta n(r)$ is also expressed as

$$\Delta n(r) = K_{\mathrm{n}}(n_{\mathrm{n}}(r) - n_0) + K_{\mathrm{e}}n_{\mathrm{e}} + K_{\mathrm{i}}n_{\mathrm{i}} \qquad (6)$$

where $n$ and $K$ show the density and specific refractive index, respectively, and subscripts e, n, and i indicate electron, neutral particle and ion, respectively, with

$$K_{\mathrm{e}} = e^2\lambda^2/8\pi^2c^2m_{\mathrm{e}}\varepsilon_0(\mathrm{m}^{-3}),$$

$$K_{\mathrm{n}} = 1.1\times10^{-29}(\mathrm{m}^{-3}),$$

$$K_{\mathrm{i}} = 3.0\times10^{-30}(\mathrm{m}^{-3}).$$

Assuming $K_{\mathrm{i}}n_{\mathrm{i}}$, $K_{\mathrm{n}}n_{\mathrm{n}}(\mathrm{r}) << K_{\mathrm{e}}n_{\mathrm{e}}$ in the plasma, Eq. (6) is rewritten as

$$n_e = \frac{\Delta n(r) + K_n n_0}{K_e}. \qquad (7)$$

## RESULTS AND DISCUSSIONS

Figure 8 shows the images of the fringe shifts taken at 3.5–6.5μs after the breakdown which corresponds to the timing after the LSD termination. Unfortunately, the interferograms during the LSD regime are too disturbed to clarify the fringe shift.

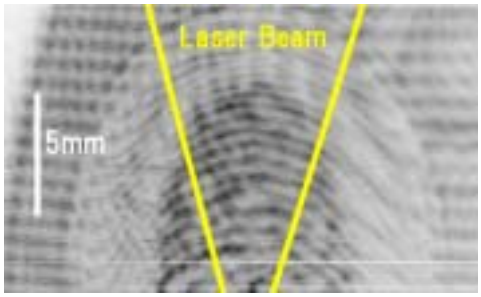


**(a) *t*=3.5μs**

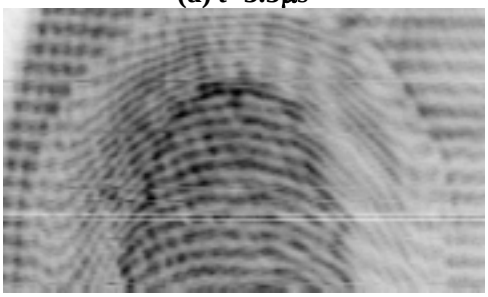

**(b) *t*=4.5μs**

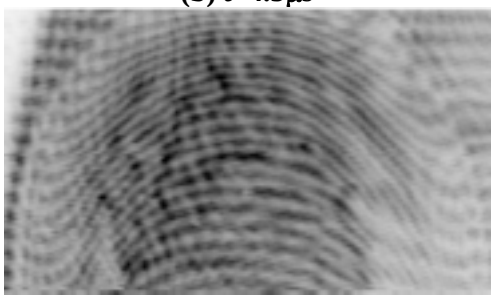

**(c) *t*=5.5μs**

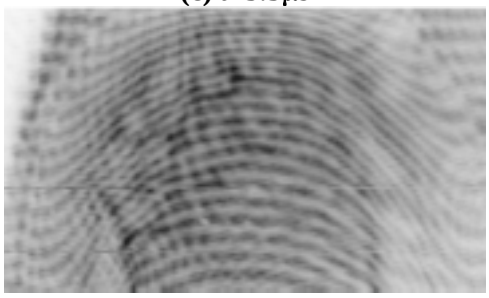

**(d) *t*=6.5μs**

**Fig. 8 Images of the fringe shifts after LSD regime is terminated.**

Figure 9 shows the two-dimensional distribution of the electron number density deduced from the fringe shift and Fig.10 shows the one-dimensional distribution along the laser axis.

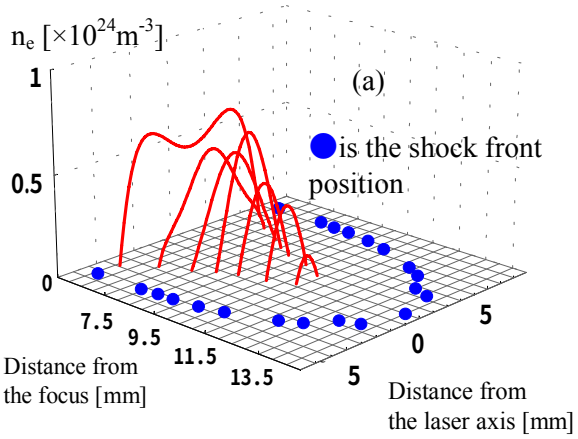


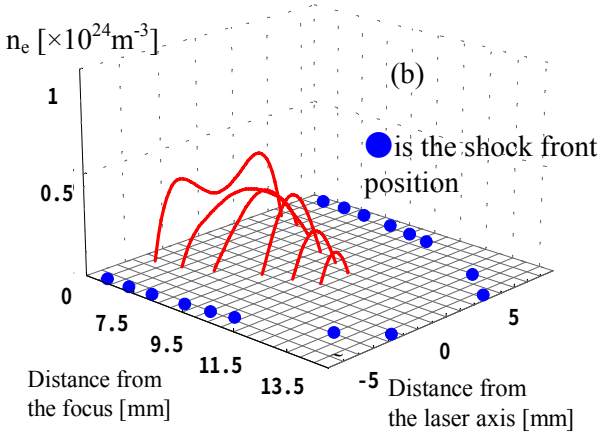


**Fig. 9 Two-dimensional electron density profile. The location of shock wave is also plotted. (a) *t*=3.5μs, (b) *t*=4.5μs.**

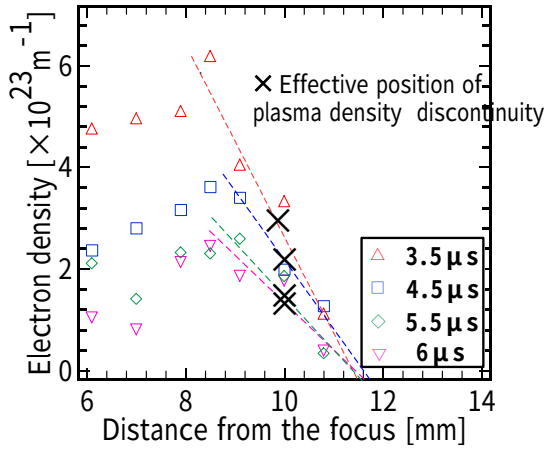


**Fig.10 One-dimensional electron density profile along the laser axis.**

Although the LSD regime has already terminated before *t*=3.5μs, electron density discontinuity was recognizable. If the location of density discontinuity is defined as the point

at half maximum of the density, it stays around $z_{LSD}$=10mm from the focus as shown in Fig. 11.

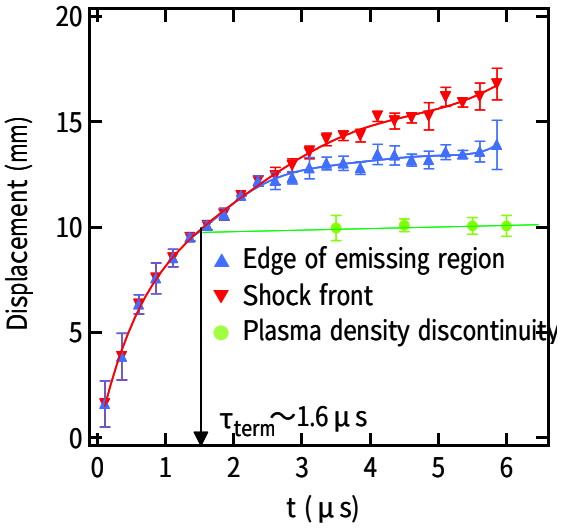


**Fig.11 History of plasma density discontinuity.**

Although the discontinuity during the LSD regime was not obtained from the interferometry, the timing of LSD termination can be determined by tracing back the discontinuity position as shown in Fig. 11. Using this value, the LSD threshold is re-evaluated as Table 2.

**Table 2 LSD threshold and fractional laser absorption. $E_i$=10J, $f$=2.2, in 1atm air.**

| Value | In Ref [3] | Present |
|---|---|---|
| $z_{LSD}$, mm | 12.0 | 10.0 |
| Threshold, MW/cm$^2$ | 3.7 ± 0.4 | 12± 1 |
| Fractional Absorption | 90% | 75% |

Depending on the difference in plasma-front definition, the threshold varied by one order of magnitude while fractional absorption by 15 %.

This information would be useful for the modeling of the plasma dynamics during the LSD regime and for the validation of computational study.

## SUMMARY

Electron density distribution behind a laser-induced blast wave has been measured by means of Mach-Zehnder interferometry. Although the density profile during the LSD regime has not been obtained from the interferometry, there were observed the density discontinuity that stayed at 10mm from the focus for several μs after the LSD termination. The position of discontinuity suggests the location where the LSD regime is terminated.

Using these data, LSD threshold was re-evaluated. As a result, depending on the difference in plasma-front definition, the threshold varied by one order of magnitude while fractional absorption by 15 %.

## REFERENCES

[1].Mori, K., Komurasaki, K. and Arakawa, Y. ”Influence of the Focusing f-number on Heating Regime Transition in Laser Absorption Waves,” Journal of Applied Physics vol.92, No.10, pp.5663~5667, 2002

[2]. Mori, K., Komurasaki, K. and Arakawa, Y. “Energy transfer from a laser pulse to a blast wave in reduced-pressure air atmospheres”, Journal of Applied Physics, Vol. 95, No. 11, pp. 5979~5983, 2004